

1 **Supplementary materials:**

2 **A case study of the highly time-resolved evolution of aerosol chemical**
3 **and optical properties in urban Shanghai, China**

4

5 Yuanlong Huang^a, Ling Li^a, Jingyan Li^a, Xinning Wang^a, Hong Chen^a, Jianmin Chen^{a,b}, Xin
6 Yang^{a,b,*}, Deborah S. Gross^c, Hongli Wang^d, Liping Qiao^d, Changhong Chen^d

7

8 ^aShanghai Key Laboratory of Atmospheric Particle Pollution and Prevention, Department of
9 Environmental Science and Engineering, Fudan University, Shanghai 200433, China

10 ^bResearch Institute for Changing Global Environment, Fudan University, Shanghai 200433, China

11 ^cDepartment of Chemistry, Carleton College, Northfield, MN 5507, USA

12 ^dShanghai Academy of Environmental Sciences, Shanghai 200233, China

13

14 Correspondence to: Xin Yang (yangxin@fudan.edu.cn)

15

16

17 **1. Size distributions of different particle types**

18 Biomass burning particles have been shown to have significant signals at $m/z +23$ (Na^+) and
19 $+39$ ($\text{K}^+/\text{C}_3\text{H}_3^+$) in the positive spectra and $m/z -26$ (CN^-) in the negative spectra. As shown in Fig.
20 2a, a 0.12 μm difference (0.28 versus 0.40 μm) was observed between the maxima of the size
21 distributions of fresh and aged biomass burning groups, which is consistent with previous studies
22 (Reid et al., 2005). Note that in the larger size range ($>0.8 \mu\text{m}$), aged biomass burning aerosols
23 still make up 15% of particles observed with the ATOFMS. Characterized by peaks of $m/z +18$
24 (NH_4^+), $+27$ (C_2H_3^+), $+39$ ($\text{K}^+/\text{C}_3\text{H}_3^+$) and $+43$ ($\text{C}_2\text{H}_3\text{O}^+$) in the positive spectra, organic carbon
25 (OC) particles account for 26.6% of all particles. A peak gap (about 0.1 μm) exists between the
26 maximum of the size distribution of fresh and aged OC types, with the peak of fresh OC type at a
27 smaller diameter of 0.48 μm . Elemental Carbon/Organic Carbon (ECOC) particles have mass
28 spectra containing a mixture of carbon clusters (C_n^+) and major OC peaks, and account for 8.7%
29 of particles observed. Both fresh and aged ECOC groups have secondary markers of (NH_4^+) and
30 ($\text{C}_2\text{H}_3\text{O}^+$). The size distribution of ECOC is bimodal. For the fresh ECOC type, the mode with
31 higher number concentration is centered around 0.28 μm and the other is around 0.64 μm . It is the
32 same situation for the aged type, however, the larger size mode is higher compared to the fresh
33 (Fig.2, 0.32 and 0.68 μm , respectively). The mass spectral pattern of the ammonium group has a
34 significant ion peak of $m/z +18$ (NH_4^+) in the positive spectra. Other peaks include OC fragments
35 of $m/z +27$ (C_2H_3^+), $+39$ ($\text{K}^+/\text{C}_3\text{H}_3^+$), $+43$ ($\text{C}_2\text{H}_3\text{O}^+$) in positive spectra and -46 (NO_2^-), -62 (NO_3^-),
36 -97 (HSO_4^-), and -125 ($\text{H}(\text{NO}_3)_2^-$) in negative spectra. The size distribution of the number fraction
37 of the ammonium type increases with the diameter.

38 Other groups including EC, dust, metal-containing, and Na-K-rich groups are named after
39 their mass spectral features, and together they account for 15.9% of all observed particles. EC
40 particles are characterized by clusters of carbon ($\text{C}_n^{+/-}$), mainly distributed in the small size range
41 (making up $\sim 50\%$ of all particle groups with diameter smaller than 0.24 μm). The particles with
42 signals from $m/z +40$ (Ca^+), $+57$ (CaOH^+), -60 (SiO_2^-), -76 (SiO_3^-), and -79 (PO_3^-) were classified

1 as dust. They are also mixed with Na, K, nitrate and sulfate. Most dust particles have diameters of
2 0.8 - 1.2 μm . Particles containing typical metal elements, e.g. Na, Mg, Al, K, V, Mn, Fe, and Pb,
3 combine to make up the metal-containing group. The Na-K-rich type has strong intensities of Na
4 and K in the positive spectra. Metal-containing and Na-K-rich particles all have nitrate and the the
5 nitrate cluster in the negative spectra. Most particles in these two groups have diameters larger
6 than 0.6 μm .

8 **2. Discussion of sulfate-, nitrate-, and ammonium- containing particle fractions**

9 Fig. S5 shows the size distributions of the number fraction of sulfate-, nitrate- and
10 ammonium- containing particles sampled with the ATOFMS in the three time periods. The
11 particles were filtered by the relative intensity of each marker using a threshold (relative peak
12 areas greater than 0.1, 0.1, and 0.05, respectively). Note that all particles containing peaks due to
13 ammonium are included here, even if they are assigned to other particle types. Sulfate particles
14 were typically found in the size range of 0.4 - 0.6 μm (about 80%). The increased sulfate in Period
15 1 likely results from the high number fraction of EC particles, as discussed in the main document.
16 The number fraction of nitrate- containing particles stayed nearly constant at around 80% for
17 particles with size larger than 0.4 μm . This indicates that about 60-80% of particles incorporated
18 more nitrite as they grew. The number fraction of ammonium-containing particles also increased
19 as the diameter grew, and the maximum number fraction got as high as 55% around 1.2 μm in
20 Period 2.

21 The size distribution trends of sulfate, nitrate, and ammonium were nearly the same in the
22 three time periods. However, the nitrate- containing number fraction was almost 20% larger in
23 Period 2 than in Periods 1 and 3 for particles larger than 0.4 μm . In addition, ammonium- and
24 sulfate- containing number fractions exceeded nearly 30% and 20% in the size range of 0.8 - 1.2
25 μm . Periods 1 and 3 shared fairly similar size distributions of number fraction in the three periods.
26 The shift of number fraction between different time periods could also be due to the influence of
27 regional transport on local aerosol chemical properties. The higher fraction of nitrate and
28 ammonium in Period 2 supports the suggestion of an input of NO_x and ammonia. Ammonia
29 prefers partitioning from the gas phase to the particle phase when RH is high. High RH during
30 Period 2 (average RH \sim 83%, see Fig. S1) promoted the partitioning of ammonia into the particles.
31 The enhancement of particulate ammonium attracts more acid into the particle phase. To
32 neutralize ammonium, sulfuric acid first gets exhausted. Then more nitrate acid partitions into the
33 particle to neutralize the excess ammonium. So in the second period both the sulfate- and nitrate-
34 containing particle number fraction was greater than in the other two periods, especially in the
35 large size range.

37 **References:**

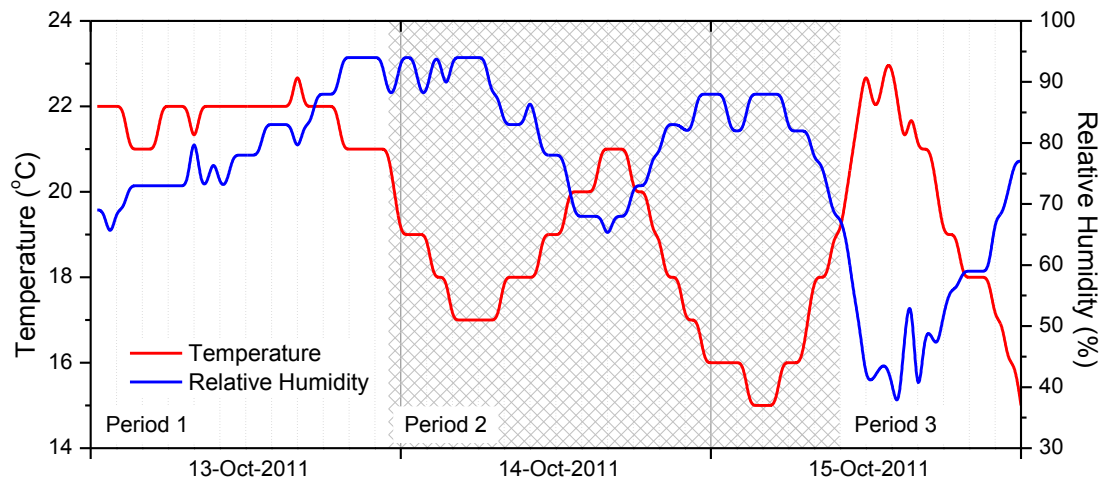
- 38 Reid, J. S., Koppmann, R., Eck, T. F., and Eleuterio, D. P.: A review of biomass burning emissions part
39 II: intensive physical properties of biomass burning particles, *Atmos. Chem. Phys.*, 5, 799-825,
40 doi:10.5194/acp-5-799-2005, 2005.
- 41 Spencer, M. T., and Prather, K. A.: Using ATOFMS to determine OC/EC mass fractions in particles,
42 *Aerosol Sci. Tech.*, 40, 585-594, doi:10.1080/02786820600729138, 2006.

1 Table S1. Results of linear regression of the scattering, absorption, and extinction coefficients
2 versus PM₁ mass loading in the four sub-periods.

3
4

Time Period	Scattering		Absorption		Extinction	
	Slope	R ²	Slope	R ²	Slope	R ²
Period 1a	1.41	0.86	0.63	0.85	2.04	0.90
Period 2a	4.31	0.93	0.86	0.95	5.17	0.94
Period 2b	1.54	0.88	0.76	0.82	2.29	0.88
Period 3a	2.80	0.77	2.07	0.91	4.87	0.93

5
6
7



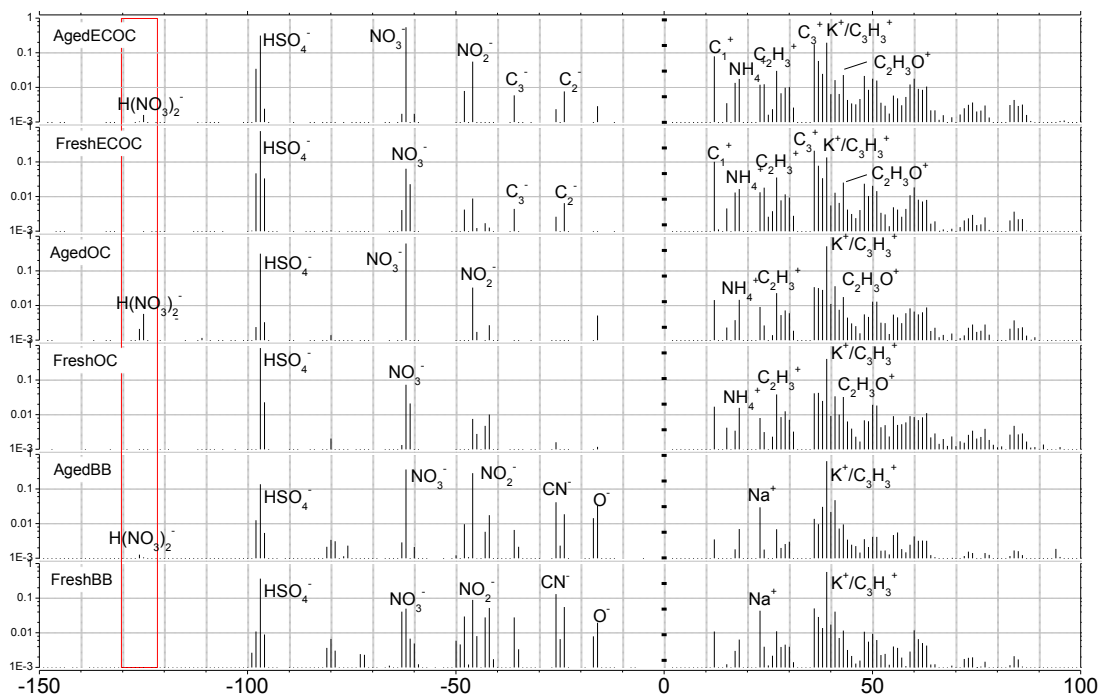
1

2 Figure S1. Temporal variation of temperature and RH over Oct 13-15, 2011 with 30-minute
 3 resolution.

4

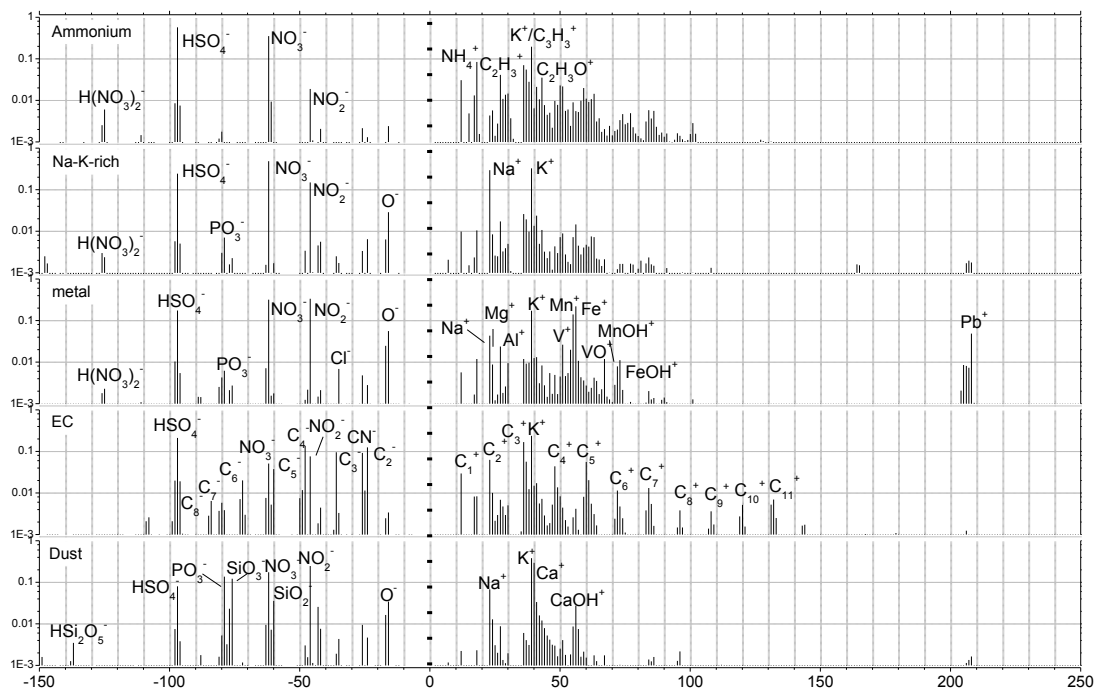
5

6



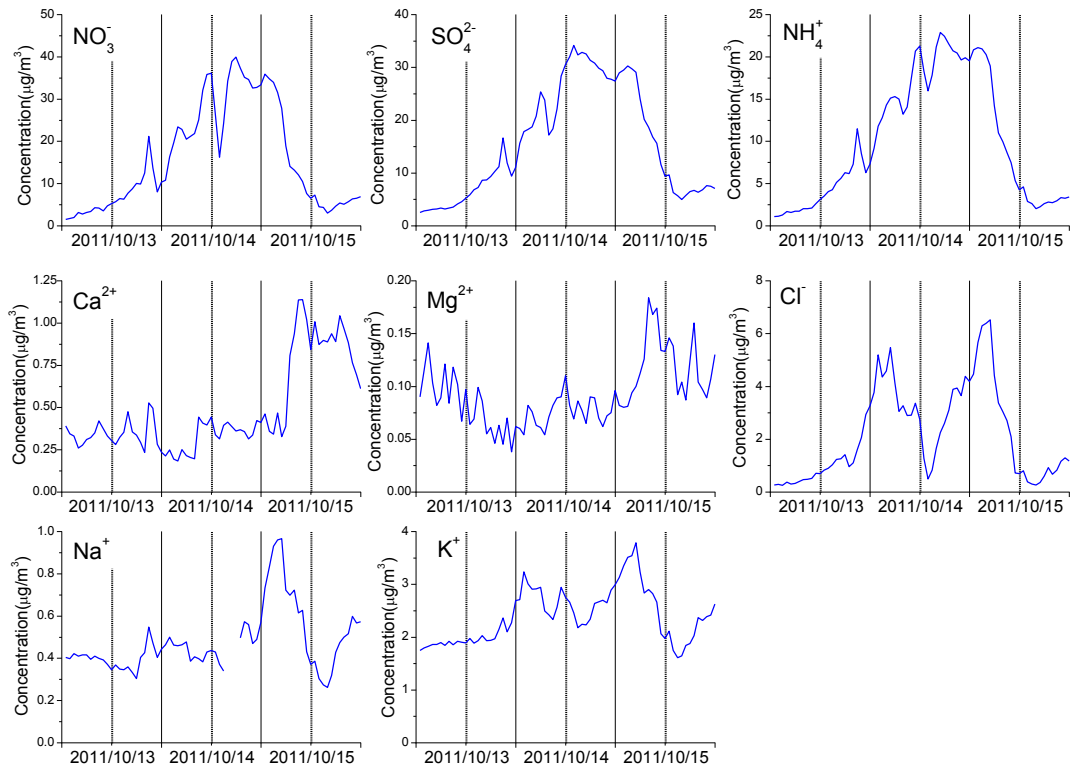
1
 2 Figure S2. ATOFMS spectra for fresh and aged biomass burning (BB), organic carbon (OC) and
 3 elemental/organic carbon (ECOC) particle types. The red box highlights the nitrate cluster ion
 4 $H(NO_3)_2^-$, a marker for aging.

5
 6
 7



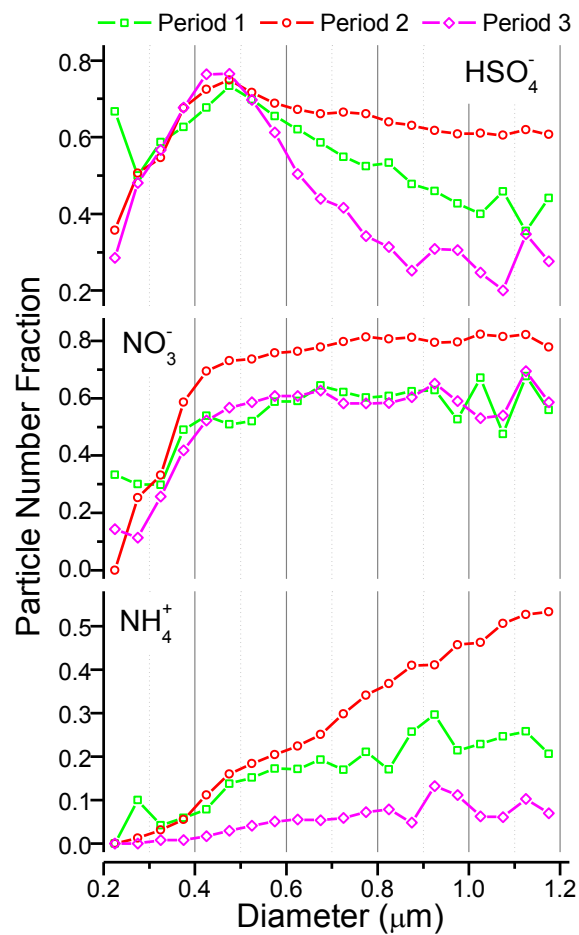
1
 2 Figure S3. ATOFMS spectra for ammonium, Na-K-rich, metal, elemental carbon (EC) and
 3 dust-containing particle types.

4
 5
 6



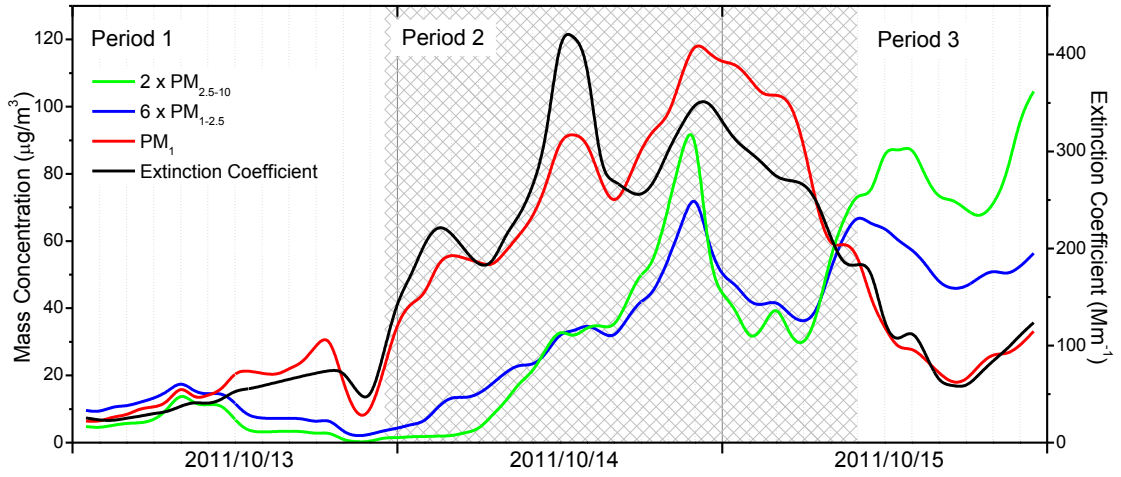
1
2
3
4
5
6

Figure S4. Temporal profiles of eight water-soluble ion mass concentrations measured by MARGA.



1
2
3
4
5
6

Figure S5. Size distributions of number fractions of particles sampled with the ATOFMS containing HSO_4^- (m/z -97), NO_3^- (m/z -62) and NH_4^+ (m/z +18) in the three time-periods.



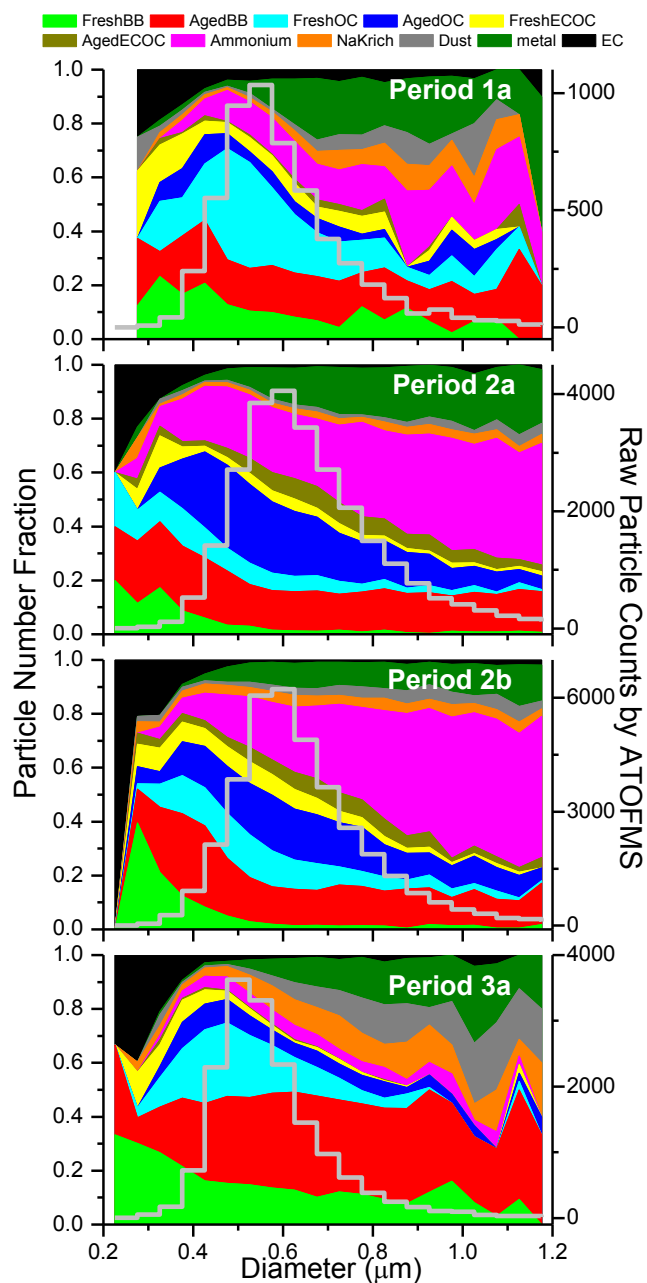
1

2 Figure S6. Temporal variations of size segregated PM mass concentrations (PM₁, PM_{1-2.5}, PM_{2.5-10})
 3 and extinction coefficient.

4

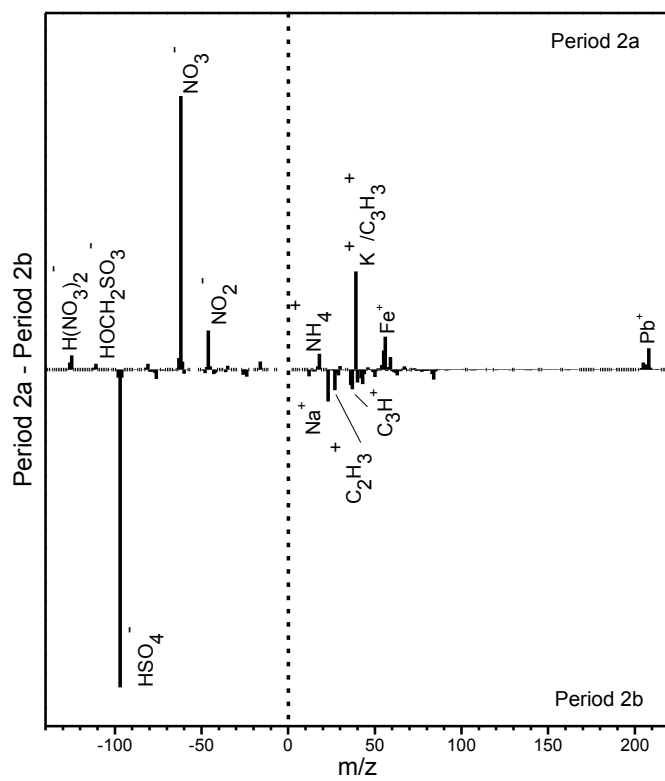
5

6



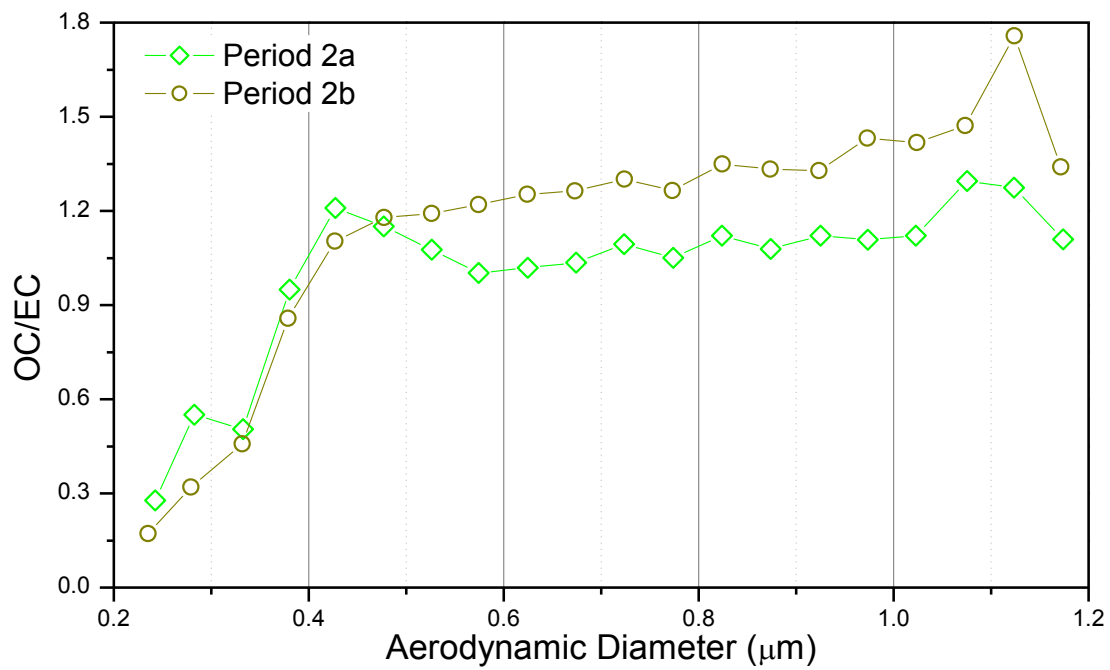
1
 2 Figure S7. Chemically resolved size distributions of different particle type number fractions and
 3 raw particle counts by ATOFMS in the four sub-periods.

4
 5
 6



1
2
3
4
5
6

Figure S8. Difference of the average mass spectra (relative peak area) of particles in Period 2a and Period 2b.



1
 2 Figure S9. Sized resolved distributions of the OC/EC ion ratio in carbonaceous particles in Period
 3 2a and Period 2b.
 4
 5